A microfiber coupler tip thermometer

Ming Ding,[1]* Pengfei Wang,[1,2] and Gilberto Brambilla[1]

[1]*Optoelectronics Research Centre, University of Southampton, Southampton, SO17 1BJ, UK*
[2]*Photonics Research Centre, Dublin Institute of Technology, Kevin Street, Dublin 8, Ireland*
* md20g09@orc.soton.ac.uk

Abstract: A compact thermometer based on a broadband microfiber coupler tip is demonstrated. This sensor can measure a broad temperature interval ranging from room temperature to 1283 ºC with sub-200 µm spatial resolution. An average sensitivity of 11.96 pm/ºC was achieved for a coupler tip with ~2.5 µm diameter. This is the highest temperature measured with a silica optical fiber device.

OCIS codes: (230.1150) All-optical devices**;** (060.2340) Fiber optics components; (060.1810) Buffers, couplers, routers, switches, and multiplexers; (060.2370) Fiber optics sensors.

References and links

1. Y. Rao, "In-fibre Bragg grating sensors," Meas. Sci. Technol. **8**, 355-375 (1997).
2. K. T. V. Grattan, Z. Y. Zhang, T. Sun, Y. Shen, L. Tong, and Z. Ding, "Sapphire-ruby single-crystal fibre for application in high temperature optical fibre thermometers: studies at temperatures up to 1500 °C," Meas. Sci. Technol. **12,** 981-986 (2001).
3. G. Coviello, V. Finazzi, J. Villatoro, and V. Pruneri, "Thermally stabilized PCF-based sensor for temperature measurements up to 1000 °C," Opt. Express **17**, 21551-21559 (2009).
4. J. Kou, J. Feng, L. Ye, F. Xu, and Y. Lu, "Miniaturized fiber taper reflective interferometer for high temperature measurement," Opt. Express **18**, 14245-14250 (2010).
5. D. Grobnic, S. J. Mihailov, C. W. Smelaser, and H. Ding, "Sapphire fiber Bragg grating sensor made using femtosecond laser radiation for ultrahigh temperature applications," IEEE Photonics Tech. Letts. **16**, 2505-2507 (2004).
6. J. Feng, M. Ding, J.-L. Kou, F. Xu, and Y. Q. Lu, "An optical fiber tip micrograting thermometer," IEEE Photonics J. **3**, 810-814 (2011).
7. J. Kou, S. Qiu, F. Xu, and Y. Lu, "Demonstration of a compact temperature sensor based on first-order Bragg grating in a tapered fiber probe," Opt. Express **19**, 18452-18457 (2011).
8. V. de Oliveira, M. Muller, and H. J. Kalinowski, "Bragg gratings in standard nonhydrogenated fibers for high-temperature sensing," Appl. Opt. **50**, E55-E58 (2011).
9. G. Brambilla and H. Rutt, "Fiber Bragg gratings with enhanced thermal stability," Appl. Phys. Lett. **80**, 3259-3261 (2002).
10. D. Barrera, V. Finazzi, J. Villatoro, S. Sales, and V. Pruneri, "Packaged optical sensors based on regenerated fiber Bragg gratings for high temperature application," IEEE Sensors Journal **12**, 107-112 (2012).
11. J. Canning, M. Stevenson, S. Bandyopadhyay, and K. Cook, "Extreme silica optical fibre gratings," Sensors **8**, 6448-6452 (2008).
12. Y. Li, M. Yang, D. N. Wang, J. Lu, T. Sun, and K. T. Grattan, "Fiber Bragg gratings with enhanced thermal stability by residual stress relaxation," Opt. Express **17**, 19785-19790 (2009).
13. L. M. Tong, R. R. Gattass, J. B. Ashcom, S. L. He, J. Y. Lou, M. Y. Shen, I. Maxwell, and E. Mazur, "Subwavelength-diameter silica wires for low-loss optical wave guiding," Nature **426**, 816-819 (2003).
14. C. Y. Chao and L. J. Guo, "Design and optimization of microring resonators in biochemical sensing applications," J. Lightwave Technol. **24**, 1395-1402 (2006).
15. G. Brambilla, "Optical fibre nanotaper sensors," Opt. Fiber Technol. **16**, 331-342 (2010).
16. G. Brambilla, G. S. Murugan, J. S. Wilkinson, and D. J. Richardson, "Optical manipulation of microspheres along a subwavelength optical wire," Opt. Lett. **32**, 3041-3043 (2007).
17. Y. Jung, G. Brambilla, and D. J. Richardson, "Broadband single-mode operation of standard optical fibers by using a sub-wavelength optical wire filter," Opt. Express **16**, 14661-14667 (2008).
18. Y. Jung, G. Brambilla, and D. J. Richardson, "Optical microfiber coupler for broadband single-mode operation," Opt. Express **17**, 5273-5278 (2009)
19. H. Guo, F. Pang, X. Zeng, N. Chen, Z. Chen, and T. Wang, "Temperature sensor using an optical fiber coupler with a thin film," Appl. Opt. **47**, 3530-3534 (2008).

#159968 - $15.00 USD Received 21 Dec 2011; revised 6 Feb 2012; accepted 14 Feb 2012; published 21 Feb 2012

20. G. Brambilla, E. Koizumi, X. Feng, and D. J. Richardson, "Compound-glass optical nanowires," Electron. Lett. **41**, 400-402 (2005).
21. F. P. Payne, C. D. Hussey, and M. S. Yataki, "Polarisation analysis of strongly fused and weakly fused tapered couplers", Electronics Lett. **21**, 561-563 (1985)
22. J. H. Wray and J. T. Neu, "Refractive index of several glasses as a function of wavelength and temperature," J. Opt. Soc. Am. **59,** 774-776 (1969).
23. C. Rodenburg, X. Lui, M. A. E. Jepson, S. A. Boden, and G. Brambilla, "Surface morphology of silica nanowires at the nanometer scale," J. Non-Cryst. Sol. **357**, 3042-3045 (2011).
24. K. O. Hill and G. Meltz, "Fiber Bragg grating technology fundamentals and overview," J. Lightwave Technol. **15**, 1263-1276 (1997).
25. A. D. Kersey, M. A. Davis, H. J. Patrick, M. LeBlanc, K. P. Koo, C. G. Askins, M. A. Putnam, and E. Joseph Friebele, "Fiber grating sensors," J. Lightwave Technol. **15**, 1442-1463 (1997).

1. Introduction

Temperature monitoring is vital for many applications in harsh environments, such as the oil and gas industries, power generation, or engine turbines. Because of their immunity to electromagnetic interference and possibility to work in contact with explosives, the use of optical fibers for temperature monitoring has been widely investigated [1-4]. Among optical fiber devices, fiber Bragg gratings (FBGs) [1, 5-12] are possibly the most common tool used for temperature sensing. FBGs inscribed in telecom optical fibers can reach temperatures T as high as 800 ^{o}C [8]. Silica optical fibers have been shown to be capable to measure temperatures in excess of 1000 ^{o}C [10-12], but they require specialty fibers and/or a long manufacturing process which includes hydrogen loading, a cumbersome grating writing equipment working with toxic gases and a relatively long post fabrication annealing. In addition to a relatively complex and expensive process, FBGs exhibit a big size (diameter d~125 µm and length L~1 cm) which restricts their application for high resolution measurements.

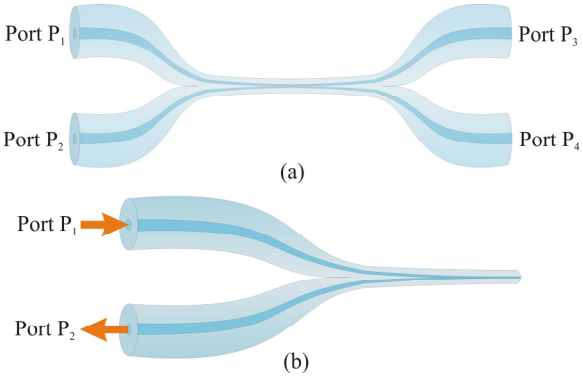

Fig. 1 Schematic of (a) a bi-conical microfiber coupler (MFC) and (b) a bi-conical microfiber coupler tip (MFCT).

In this paper, a compact thermometer based on a microfiber coupler tip (MFCT, Fig. 1(b)) is presented. Since a seminal paper was published in 2003 [13], optical microfibers and their related devices have attracted increasing attention because of their wide range of applications which include, amongst others sensors [14, 15], particle manipulation [16] and modal filters [17]. In 2009, Jung et al. [18] demonstrated a broadband singlemode bi-conical 2×2 microfiber coupler (MFC, Fig. 1(a)) with specifically designed transition regions which effectively suppress any high order mode present at the input fiber and provide efficient power splitting of the fundamental mode at the two output ports. The MFC was manufactured by laterally fusing and tapering two twisted optical fibers. By controlling the taper transition profiles and the MFC minimum diameter in the uniform waist region, singlemode operation over the wavelength range 700-1700 nm was demonstrated. While fused optical fiber couplers have found many applications in optical communication due to its high performance and low

#159968 - $15.00 USD Received 21 Dec 2011; revised 6 Feb 2012; accepted 14 Feb 2012; published 21 Feb 2012

cost, its application to temperature monitoring [19] related only to low T (below 100 °C) and resulted in low responsivity. In this paper, a microfiber coupler with minimum diameter of ~2.5 µm was chosen to ensure high sensitivity, high spatial resolution and an adequate rigidity for the thermometer head, even if this resulted in slightly multimode guidance. In the coupling region, supermodes with different propagation constants provide a continuous change in the power distribution along the coupler cross section, which results in a different power splitting at the output ports for different optical paths. The modes optical paths depend both on the coupling region length and its refractive index; since both depend on the surrounding environment, and in particular on its temperature, the MFC can be used as a highly sensitive thermometer. In conventional optical fiber couplers, the periodicity in the coupler transmission spectrum is typically few hundred nanometers, therefore a small temperature increase results in a proportionally small shift, thus small responsivity [19]. On the contrary, in MFCs, this periodicity is of the order of few/tens of nm: a wavelength shift of few nanometers generally results in large changes in the transmitted power at a specific wavelength, thus a high responsivity. Moreover, since this component is made of pure silica, which softens at T~1680 °C, it can potentially reach very high temperatures.

2. Microfiber coupler thermometer fabrication

The MFCT thermometer was manufactured by cutting a MFC (Fig. 1(a)) with a ceramic cleaver into two equal parts at the center of the minimum waist region. A MFC comprises two conical transition regions, a central uniform waist region and four input/output ports: light injected from ports P_1 or P_2 exits MFC from ports P_3 and P_4. In the MFCT, light launched from port P_1 is partially reflected by the flat surface of the tip and can be measured at port P_2. In these experiments, a low-loss MFC was fabricated from two standard telecom optical fibers (SMF-28, Corning, NY, USA) using the microheater brushing technique [20]. The lengths of tapered and uniform waist regions were ~25 mm and ~6 mm, respectively. Fig. 2(a) shows the scanning electron microscope (SEM) image of the MFCT: the minimum diameter and length of the uniform waist region were ~2.5 µm and ~3 mm. The MFCT spectral characterization was carried out connecting a supercontinuum (SC) source (Fianium Ltd, Southampton, U.K.), with emission over the wavelengths range 450-1800 nm, to port P_1 and an optical spectrum analyzer (OSA) (AQ6317, Yokogawa, Japan) to port P_2. The reflection spectrum at room temperature is presented in Fig. 2(b) and shows the multipeak pattern of optical fiber couplers. On the contrary of conventional fused couplers made from telecom singlemode optical fibers, the pattern is not limited to the 1250-1750 nm range, but covers the whole investigated wavelength range 700-1700 nm.

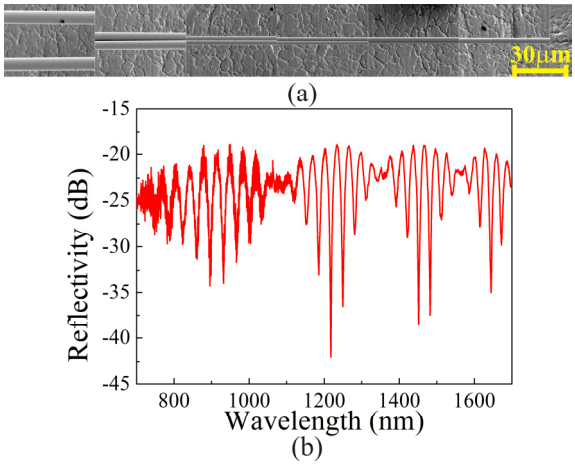

Fig. 2 (a) SEM images of the MFCT. Single microfiber diameter and uniform region length are ~2.5 µm and ~3 mm, respectively; (b) MFCT reflection spectrum at room temperature.

#159968 - $15.00 USD Received 21 Dec 2011; revised 6 Feb 2012; accepted 14 Feb 2012; published 21 Feb 2012

A long wavelength modulation is superimposed to the coupler spectrum and it is due to difference of coupling coefficient for *x* and *y* polarizations.

3. Temperature dependence of the MFCT

The MFC output can be predicted by assuming that power exchange at the output ports occurs as a result of the interference between the lowest-order symmetric and antisymmetric modes of the waveguide formed by the whole of the cross section of the fused region. From Fig. 2(a), the MFCT can be assumed to be a "weakly fused" coupler, approximated by two touching cylindrical waveguides (the Fig. 3 inset shows a schematic of coupler cross section in this approximation). Since the original fiber cores have a negligible size, they can be ignored and the coupling coefficients C_x and C_y for the *x* and *y* polarization are given by [21]:

$$C_x = \frac{2^{3/2}(n_1^2 - n_0^2)^{1/2} U_\infty^2 (2n_1^2 V + 1)}{n_1^3 a(\sqrt{\pi}) V^{7/2}} \tag{1}$$

$$C_y = \frac{2^{3/2}(n_1^2 - n_0^2)^{1/2} U_\infty^2 (2n_1^2 V - 1)}{n_1^3 a(\sqrt{\pi}) V^{7/2}} \tag{2}$$

where n_1 and n_0 are the refractive indices of silica and air, a is the diameter of one of the microfibers, $U_\infty = 2.405$ and $V = [(2\pi a)/\lambda](n_1^2 - n_0^2)^{1/2}$.

If light entering the input port P_1 in the MFC is unpolarized, the normalized power at the output port P_4 can be described by:

$$P_4 = \frac{1}{2}\{1 - \cos[(\overline{C_x} + \overline{C_y})L]\cos[(\overline{C_x} - \overline{C_y})L]\} \tag{3}$$

where L is the coupling length of MFC which includes the waist uniform region and the transition region and $\overline{C_x}$ and $\overline{C_y}$ are the values of Eq. (1) and Eq. (2) averaged over the whole length where coupling occurs. Because of the large modal size and the relatively small overlap, the contribution of the transition regions to the average coupling coefficients is small/negligible.

In the MFCT, light launched from port P_1 is reflected by the tip and the power emerging from P_2 is proportional to P_4 in Eq. (3):

$$P_2 = \left(\frac{n_1 - n_0}{n_1 + n_0}\right)^2 P_4 \tag{4}$$

Equations. (1-4) show that the output power depends on the wavelength λ and on three factors (refractive index n_1, coupling length L and coupler radial size $2a$), which are temperature dependent.

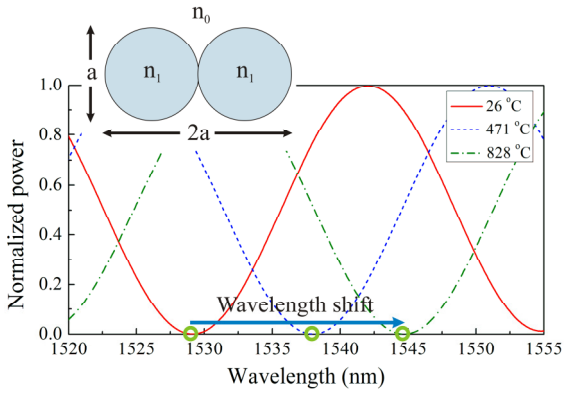

Fig. 3 The output power from port P_2 at 26 ºC, 471 ºC and 828 ºC. Inset: MCFT cross section in the "weakly fusing" approximation.

#159968 - $15.00 USD Received 21 Dec 2011; revised 6 Feb 2012; accepted 14 Feb 2012; published 21 Feb 2012

The temperature dependence of the MFCT output spectrum was evaluated assuming the refractive index of silica at λ~1530 nm at T=26 ºC, 471 ºC and 828 ºC to be 1.44444, 1.44961 and 1.45352 [22], respectively. The diameter of each microfiber in the uniform region and the length of the uniform region (2.5 µm and 3 mm, respectively) were assumed to expand with an average coefficient 5.5×10^{-7} ºC^{-1}. Fig. 3 shows the output power variation at three different temperatures. The resonance peak shifts 15.5 nm when T is increased from 26 ºC to 828 ºC, with an average responsivity of 19.3 pm/ ºC.

4. MFCT Characterization

4.1. Responsivity

Sensor characterization was carried out using the same microheater (NTT-AT, Tokyo, Japan) used to fabricate the MFC, as it can reach temperatures in excess of 1700 ºC. The MFCT was inserted to the microheater center (Fig. 4(a)) and the reflection spectra were recorded at different T. The microheater temperature was changed by increasing the current flowing into the microheater from 0.4 A to 2.8 A in steps of 0.2 A. Measurements were taken every 15 minutes to ensure a stable temperature. The microheater response was proposed in ref. [23] and it is reported in Fig. 4(b) to include small currents. Figure 4(c) shows the spectral shift of the peak at 1219 nm in Fig. 2(b) for increasing currents. When the driver current is increased, the temperature increases and the peak redshifts to long wavelengths, as predicted by simulations in Fig. 3.

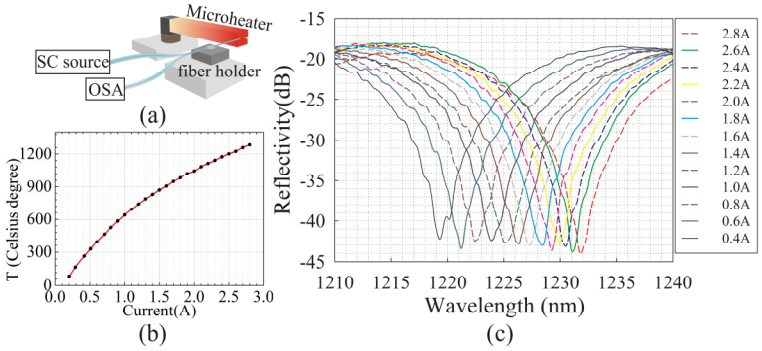

Fig. 4 (a) MFCT characterization set-up; (b) relation between the driver current and temperature; (c) reflection spectra of the peak at 1219 nm in Fig. 2(b) when the driver current increases from 0.4 A to 2.8 A by steps of 0.2 A.

The sensor responsivity (also called sensitivity) R is defined as the wavelength shift associated to a temperature change. In order to minimize the measurement error, spectra were fit with Lorentzian functions and the fit peak wavelength was used to calculate the wavelength shift. An average R~11.96 pm/ºC was achieved in the temperature range ~247 ºC to ~1283 ºC, comparable to the value obtained for FBG thermometers at lower T [24, 25]. The possible explanation for the difference between the theoretical calculation and experimental measurement could be the unperfected weakly fused coupler structure, the measured wavelength difference and the refractive index error. The sensor resolution was estimated to be ~0.836 ºC for an OSA resolution of 0.01 nm. Better resolutions can be potentially achieved with more spectral data points for the Lorentzian fitting and/or better signal/noise (i.e. spectral averaging).

4.2. Repeatability

The MFCT thermometer repeatability was measured recording spectra for increasing and decreasing temperatures with an interval of one hour. The wavelength shift with the temperature is shown in Fig. 5: data from the two curves fit very well within 3 ºC, showing that the MFCT thermometer has good repeatability.

#159968 - $15.00 USD Received 21 Dec 2011; revised 6 Feb 2012; accepted 14 Feb 2012; published 21 Feb 2012

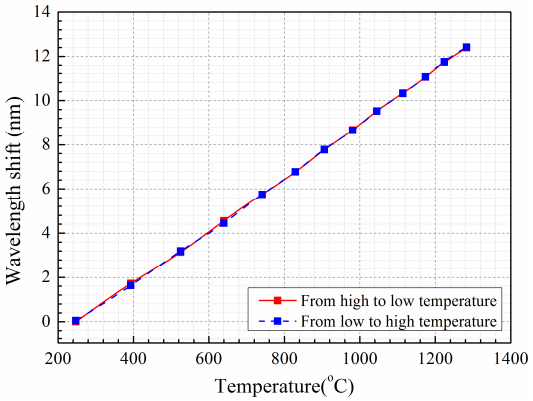

Fig. 5 Wavelength shift dependence on the microheater temperature. The red solid curve and the blue dash curve report measurements for decreasing and increasing temperatures, respectively.

4.3. 2D spatial resolution

In order to demonstrate the sensor high 2D spatial resolution, measurements were carried out as shown in Fig. 6(a). A Nickel-Chromium (Ni-Cr) wire with ~500 μm diameter was heated exploiting its Ohm effect. Spectra were recorded every 125 μm at a distance of ~250 μm from the Ni-Cr surface along the tangential direction: the peak shift of Lorentzian fitting spectra variation with the MFCT position is presented in Fig. 6(b), with the origin taken as the central axis of the wire. A sharp peak with a full width at half maximum (FWHM) of ~1150 μm was observed. FWHM is larger than the wire size as the temperature gradient becomes smaller for increasing distances from the heated wire, thus the FWHM is bound to increase for increasing distances from the wire.

A wavelength shift of 1.19 nm was recorded at the wire center corresponding to a temperature difference of ~99 ºC. If heat is assumed to be dissipated by conduction in air, the T profile can be easily found from the solution of Fourier law in stationary state, which leads to Laplace equation: $\nabla^2 T = 0$. The solution provides the following equation along the line used for measurement:

$$T = C_1 * \ln[x^2 + (500\mu m)^2]^{1/2} + C_2 \qquad (5)$$

where C_1 and C_2 are constants related to the heat transfer density and wire diameter, x is the distance from the closest point in the measurement.

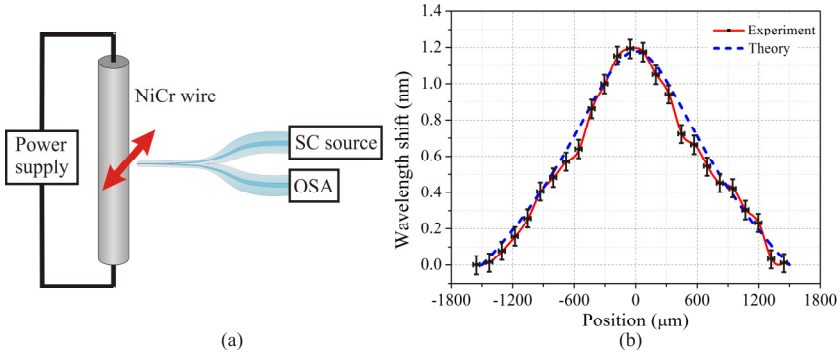

Fig. 6 (a) Experimental set-up used to demonstrate the MFCT 2D spatial resolution; (b) sensor response when the MFCT was scanned along the tangential direction of the Ni-Cr wire at ~250 μm from the wire surface. The red solid and the blue dash curves are the experiment results and the curve expected from heat transfer equation, respectively.

#159968 - $15.00 USD Received 21 Dec 2011; revised 6 Feb 2012; accepted 14 Feb 2012; published 21 Feb 2012

A reasonably good fit between Eq. (5) theory and experimental data shown in Fig. 6(b) occurred for C_1=-284.7 and C_2=1114.7, respectively. The small difference between two curves can be associated to the tip head movement, to the wire temperature fluctuations during the measurement and to the stage movement error. The measurement errors are shown with error bars.

The shift recorded in Fig. 6(b) is related to the temperature profile of the coupling region in the sensor, thus the presented data is influenced by the temperature profile over the sensor longitudinal direction. A reduction of the sensitive area length can improve the resolution along the sensor longitudinal direction and allow for high resolution 3D measurements.

5. Conclusions

In summary, a compact temperature sensor which uses a MFCT for high-*T* sensing with high 2D spatial resolution has been demonstrated. This device exploits the temperature dependence of intermodal coupling in the coupler uniform waist region. The thermometer had a responsivity of 11.96 pm/ºC and an operational range exceeding 1200 °C (from room temperature to ~1283 ºC). A measurement with a sub-200 μm 2D spatial resolution has also been demonstrated. Because of the small coupler cross section, the theoretical device resolution is limited by the Raleigh criterion, meaning that measurements with resolutions smaller than 5 μm can be possible. Since the MFCT is made from pure silica and silica softens at ~1680 °C, this device could potentially work at temperatures well in excess of 1283 ºC, which is the highest temperature recorded so far with a device made from a conventional telecom optical fiber. MFCT offers several advantages, including compactness (few μm in diameter), high temperature measurement capabilities, high responsivity, high spatial resolution, easy connection with other fiberized optical components, simple fabrication and low cost. Since the measured temperature is the average temperature of the intermodal coupling region, high resolution 3D measurements could be made possible by reducing the length of the sensitive area. Moreover, although response time measurements have not been carried out, because of the reduced volume this device is expected to have a response time comparable/better than that observed in thermometers based on optical fiber gratings. The possibility to have high resolution *T* measurements could find useful applications in biology, medicine and material science.

Acknowledgements

GB gratefully acknowledges the Royal Society (UK) for his University Research Fellowship.

#159968 - $15.00 USD Received 21 Dec 2011; revised 6 Feb 2012; accepted 14 Feb 2012; published 21 Feb 2012